



Energy, Mines and
Resources Canada

Énergie, Mines et
Ressources Canada

CANMET

Canada Centre
for Mineral
and Energy
Technology

Centre canadien
de la technologie
des minéraux
et de l'énergie

A CRITICAL REVIEW OF

"SIZE DISTRIBUTIONS OF FLOCCULATED PARTICLES:

APPLICATION OF ELECTRONIC PARTICLE COUNTERS"

Published in "Environmental Science and Technology"

N.E. Andersen

Western Research Laboratory

January 1979

14 pp
ENERGY RESEARCH PROGRAM

ENERGY RESEARCH LABORATORIES

REPORT ERP/ERL 79-17(TR)

ERP/ERL 79-17 (TR)

A CRITICAL REVIEW OF
"SIZE DISTRIBUTIONS OF FLOCCULATED PARTICLES:
APPLICATION OF ELECTRONIC PARTICLE COUNTERS"

Authors: Gordon P. Treweek and James J. Morgan

Published in "Environmental Science & Technology"
vol 11, No. 7, July, 1977

by
N.E. Andersen*

Our laboratory is presently involved in extensive studies of fine particles and as such, the process of flocculation and/or the behaviour of flocculated particles is of major interest.

We have operated a Coulter Counter (Model TA II) in our laboratory for about two years but have not yet applied it to the analysis of aggregates. Consequently, the above paper (Appendix) is particularly welcome as it provides useful insight into the problems associated with such analyses.

I would however, like to present the following observations on this paper.

1. The primary concept of the paper is that a conservation of volume condition must exist between the unflocculated and flocculated state. The system response to aggregates is shown to be reduced by the nature (porosity) of the aggregates and as such, a correction factor (> 1) must be applied, the maximum value of which was determined experimentally from an asymptotic porosity value which preserves the above mentioned conservation of volume condition.

*Mineral Processing Scientist, Western Research Laboratory, Energy Research Laboratories, Canada Centre for Mineral and Energy Technology, Dept. of Energy, Mines & Resources; Edmonton, Alberta, Canada

In this case the correction factor (K) to be applied is given by:

$$K = \frac{1}{\sqrt[3]{1 - [1.5 \log (d/d_0)]^{1.9}}} \quad \text{and has a maximum value of } \sqrt[3]{2} \text{ at}$$

maximum d/d_0 of 2.9, where d = equivalent spherical diameter of aggregate, d_0 = singlet diameter.

It is not clear however, from the article, how this limiting porosity value ($f = 0.69$) was obtained. The Figures 3B - 6B show only differential volume distribution. Do the areas under these curves represent total particulate volume? No units of volume are indicated on the ordinate axis of these graphs; from the magnitude, I assume particle volume is in μm^3 .

The shift in both particle count and particle volume to larger sizes is clearly indicated from the graphs presented. However the total particulate (cell) volume per unit volume of suspension and its conservation by applying equations 13, 15 and 16 to raw Coulter data is not indicated. It is apparent that analyses have been carried out on known volumes of suspension and therefore I feel that graphical presentation of particulates/unit volume (1) before flocculation and (2) after flocculation, a) before applying porosity correction and b) after applying correction, would have been informative.

It is stated (p. 711 column 1) that E. coli cell concentration was diluted to 2.5×10^5 cells/ml, at which the 11- μm aperture would not require coincidence correction, yet in graphs 3A to 6B it is stated that initial particle count was in the range of 2.5×10^7 /ml.

A useful approximation for coincidence loss is:

$$C = \frac{ND^3}{8}, \quad \text{where}$$

C = coincidence loss in %

N = observed count per ml

D = aperture diameter in mm

Thus a cell concentration of 2.5×10^7 /ml would result in a coincidence loss of 4.2%, an apparently acceptable loss and dilution to 2.5×10^5 cells/ml does not appear to have been necessary.

3. The authors stated that particles below $1.13 \mu\text{m}$ e.s.d. could not be detected by the $11 \mu\text{m}$ aperture because of background electronic noise. This detection limit appears to be very high in view of our experience, wherein we are able to routinely analyze particles down to $< 0.4 \mu\text{m}$ (without background correction) using a $15 \mu\text{m}$ aperture tube. Is this high level of background noise inherently associated with the PHA-MCA system or is it a result of external interferences?

4. The presence of larger aggregates resulting from flocculation with high molecular weight polymers is attributed to their increased shear resistance. I do not believe this to be the case. If shearing forces are responsible for the absence of large aggregates with low molecular weight polymers, the shear must result from either stirring or from passing through the aperture. Presumably, the highest shearing forces (velocity gradients) are encountered when the aggregates pass through the aperture, where flow velocities are of the order of 5m/sec . The authors state that "the aggregates did not appear to fragment as they passed through the aperture in spite of the high shear forces encountered there".

We have found that low molecular weight polymers form smaller aggregates, even in the absence of significant shearing forces. It has been found that high molecular weight polymers, on the other hand, produce larger aggregates presumably because of their increased molecular size which promotes a higher degree of bridging between particles and consequently larger aggregates.

5. The following apparent errors were observed:

A. Should equation (9) p. 710 not read:

$$\Delta R = 4 p_0 d^3 \left\{ 1 - [1.5 \log (d/d_0)]^{1.9} \right\} / 1.5 \pi D^4$$

B. Figure 3A, p. 712. Should the caption not read:

Differential number distribution of E. coli aggregates with no added flocculant.

C. p. 712, last sentence. Should this not read:

Aggregates in the $10\text{-}20 \mu\text{m}$ range are equivalent to $455\text{-}3640$ singlets/aggregate.

D. Figures 3A - 6B.

Is the correct term not flocculant; flocculent being a descriptive term (1).

REFERENCE

- (1) A Dictionary of Mining, Mineral and Related Terms; U.S.B.M., Washington, 1968, p.442.

APPENDIX

Size Distributions of Flocculated Particles: Application of Electronic Particle Counters

Gordon P. Treweek^{1*} and James J. Morgan

Division of Engineering and Applied Science, California Institute of Technology, Pasadena, Calif. 91103

■ A review of currently used particle size analyzers for liquid suspensions reveals that only the electronic resistance devices measure the particle volume directly. Although the electronic analyzer's ability to measure singlet particles is well documented, two major difficulties occur in measuring aggregate size distributions in flocculating systems. Since electronic counters measure only the particulate matter within a floc, the equivalent spherical diameters so recorded do not coincide with the microscopically observed diameters. Also, evidence exists that electronic counters only partially measure the total particulate matter within an aggregate because of the physical separation which exists between the component singlets. In this research the recorded electronic response is correlated with the aggregate porosity, and equations are derived to enable the investigator to correct for porosity effects. The new relationships between aggregate size and counter response are based on a modification to the existing equations for the passage of a singlet particle through the measuring aperture. The validity of the new equations is established in a flocculating *E. coli*-polyethyleneimine suspension in which the complete particle size distribution is recorded. Since a conservation of volume condition must exist between the unflocculated and flocculated state, this condition is used to determine the limiting porosity value in well-flocculated suspensions.

Within the past 10 years, several new experimental methods have been developed to measure the extent of aggregation produced in coagulation/flocculation treatment processes. These methods enable the researcher to quantitatively record the effectiveness of varying the flocculent type and dose, the velocity gradient and time of mixing, the number of mixing chambers and type of stators, and other factors known to influence the coagulation/flocculation treatment process. In the past, many experimental methods were either qualitative in degree or measured only the phase separation aspect of the flocculation process, which often led to errors when laboratory bench tests were scaled up to full-size facilities. To some extent, the emphasis on measurement of phase separation alone biased the investigator toward improvement of the physical parameters of the system, at the expense of possible chemical alterations which would enhance the destabilization phase of coagulation. The new aggregate measurement techniques enable the researcher to investigate thoroughly and accurately the destabilization of suspended colloidal matter as it occurs, in lieu of measuring just the end result: phase separation.

Table I summarizes the experimental techniques which are currently available to record the extent of aggregation of particulate matter in liquid suspensions. Each technique is characterized by some disadvantages, which are often more pronounced in the measurement of aggregate size distributions than in the measurement of singlet size distributions. Some techniques offer significant advantages in particular applications, such as the ability of the light interruption technique to operate in the continuous flow, real-time mode (1) or of the membrane refiltration technique to rapidly

evaluate changes in the specific surface area of aggregates utilizing simple, inexpensive equipment (2-4). With the exception of the electrical resistance method which measures aggregate volume, all the techniques measure either the aggregate cross-sectional area, or a parameter such as sedimentation velocity, which depends directly on the aggregate cross-sectional area. Because of its unique ability to measure aggregate volume, the electronic counting and sizing technique was selected for further study.

The electronic particle counting and sizing technique appears ideally suited to evaluating changes in the number distribution of suspended particulate matter brought about by the addition of coagulants in a water or wastewater system. Since the aggregate volume is measured directly, a differential volume distribution can be readily determined, thereby providing an indication of the equilibrium aggregate volume attainable under selected flocculation conditions. The detectable size range for the method (0.5-900 μm) enables the investigator to evaluate the extent of orthokinetic flocculation, which primarily affects particles greater than 1 μm in diameter (5). Because of the difficult experimental procedures involved in recording a complete size distribution by this method, and because of the cost of the data acquisition and data reduction equipment, electronic particle sizing is limited to laboratory experiments. However, particle size distributions evaluated by this technique have been correlated with turbidity and refiltration rate measurements, both of which are currently used in treatment practice (4).

The electronic particle counting and sizing technique has been successfully employed with suspensions of singlet particles for 20 years. Results have been verified with respect to count via hemacytometers and with respect to size via calibrated oculars, grids, or known particles (6-9). However, no effort has been made to verify whether the electronic sizing technique can be successfully used to count and size unflocculated flocs of primary particles. Consequently, research was undertaken to determine if the principles of operation of the electronic particle counter could be extended to flocculated particles similar to those found in water and wastewater treatment operations.

Prior Applications of Electronic Particle Counting

In 1956 W. H. Coulter announced the development of a precise counter for discrete microscopic particles (10). This counter found immediate application in many medical and industrial situations. Mattern et al. (6) used a 100- μm aperture to measure the number and size of red blood cells; they found the instrument counts to be more accurate than those obtained via the hemacytometer and deduced a linear relationship between pulse height and particle volume. Kubitschek (7,8) extended the instrumental technique to bacteria with the use of a 20- μm aperture, and also found a strictly linear performance of the counter in response to particle volume, as long as the particle diameter was greater than 10% and less than 40% of the aperture diameter. Further experimental improvements, coincidence counts, background reduction, and size distributions for discrete particles, are discussed in the work of Wachtel and LaMer (9).

Higuchi et al. (11) were among the first to study the aggregation of particles (in this case, an oil-in-water emulsion) with a Coulter counter. They prepared a relatively monodis-

¹Present address, James M. Montgomery, Consulting Engineers, Inc., 555 E. Walnut Street, Pasadena, Calif. 91101.

persed emulsion, with droplets of about 1 μm diameter, by an electrical dispersion technique and then measured the aggregation/deaggregation of this emulsion with varying concentrations of dioctyl sodium sulfosuccinate (AOT). Fortunately, their emulsion particles coalesced upon contact; therefore, detection of aggregated particles was no different from detection of singlets.

Further improvements in measuring the particle size distribution of aggregating systems included the introduction of the multiaperture analysis procedure (12, 13) and the application of a pulse height analyzer (PHA) with multichannel storage (MCA) (11, 15).

The accuracy of the electronic counter in enumerating and sizing singlets within the size range 10–40% of aperture diameter has been verified with both the optical and electron microscope. In the case of particle aggregates, only qualitative checks have been made on aggregate sizes recorded by the counter. The first indication that the electronic counter may

not accurately record the aggregate size was noted by Camp (16) in his analysis of a series of experiments by Hannah et al. (17) who evaluated the floc strength of a kaolin-alum floc in a modified Couette mixing apparatus which contained a 70- μm aperture capable of recording six size ranges from 1.3 to greater than 9.0 μm . Using their data, Camp estimated the volume fractions for mixing times of 1, 5, and 10 min to be 4.7, 3.0, and 2.2 ppm, respectively. The initial volume of clay and Al_2O_3 was estimated at 4.3 ppm, and the velocity gradient was set at 50 s^{-1} to promote rapid floc formation without settling. Camp attributed the recorded loss of volume during flocculation to the dissolution of kaolin within the system.

Camp (18) attempted a similar volumetric analysis of the data of Ham and Christman (14), in which the formation of silica floc with alum was studied with a 240- μm aperture. Camp determined that the volume concentration increased from 1.6 to 3.6 ppm as the flocculation proceeded from 10 to 36 min. This result is expected since the 240- μm orifice re-

Table I. Experimental Techniques to Determine Extent of Aggregation

Technique	Property measured	Size range, μm	Description of process	Disadvantages
Optical Microscope	Length/width	0.2–400	Visual observation and comparison of aggregates with calibrated slide or lens	Time consuming and laborious; judgment errors in estimating size
Microscope automated	Length/width	0.5 and up	Microscope slide or photograph electronically scanned to record aggregate images	Time consuming; expensive peripheral equipment
Light scattering (also laser scattering)	Light intensity	2–500	Intensity of light energy scattered from particle in direction of sensor	Varying refractive indices of heterogeneous particles; multiple scattering effects in aggregates; criticality of sensing angle
Light interruption	Light blockage	2–9000	Reduction of light intensity on sensor as aggregate passes by detector	Opacity of fluid medium; identical refractive indices of particle and fluid
Spectrophotometric	Light intensity	0.002 and up	Observation of reduction in light intensity upon passing through suspension of aggregates (turbidity)	Complicated relationship between turbidity and size, i.e., $T = \sum n_i \pi r_i^2 K_i$, where n_i = number of particles of radius r_i , K_i = extinction coefficient which is function of relative refractive index, wavelength, and radius
Visual	Length/width	20 and up	Observation of appearance and size of aggregates	Time consuming and laborious; judgment errors in estimating size
Sedimentation/filtration Gravity sedimentation	Velocity	0.1–100	Observation of steady-state aggregate velocity through suspending media	Density and shape factors of aggregate unknown; time-consuming and laborious
Centrifugal sedimentation	Velocity	0.02–10	Observation of steady-state aggregate velocity as centrifugal force drives aggregate through suspending media	Density and shape factors of aggregate unknown; shearing and distortion of aggregates
Membrane refiltration	Filterability	0.45 and up	Formation of filter cake on 0.45- μm filter by filtering suspension, followed by refiltration of filtrate through filter cake	Filtration time a function of both filter cake porosity and specific surface area of aggregates
Electronic Electrophoretic mobility	Velocity	0.1–100	Observation of steady-state aggregate velocity as potential difference draws aggregate through suspending media	Density and shape factor of aggregate unknown; velocity a function of both unbalanced charge density and aggregate diameter
Electrical resistance	Resistivity	0.5–900	Aggregate passes through aperture causing resistance change in electrolyte between two electrodes. Resulting voltage pulse is proportional to aggregate volume	Blocking of aperture; expensive peripheral equipment

solves only the upper end of the total particle size distribution, i.e., due to background noise, small agglomerates and individual silica particles are not detected in the initial size distribution measurement. With the 240- μm aperture, large aggregates are detected, but the loss of small particles within the total size distribution goes unnoticed. Using the data of Ham and Christman, Camp calculated the water content of the silica-alum floc to range from 74 to 99.9%.

Ham (19) recognized that the aggregate sizes recorded by the electronic counter for a coagulated silica suspension did not correspond to the sizes measured optically. The discrepancy between the two methods was attributed to either aggregate distortion upon passing through the orifice of the counter or to the large porosity of the aggregate, which resulted in a larger visual size than justified by the particulate content. Ham alleviated the first problem by using a large (240 μm) aperture, and recognized that the aggregate porosity prevents a direct comparison between sizes determined by the counter (which measures only the particulate content) and microscopic observation (which measures total floc size including entrapped electrolyte).

Recently, Neis et al. (20) recorded a decrease in the specific resistance of polystyrene latex agglomerates during electronic counting experiments. This decrease was attributed to the higher electrolyte content of the aggregates and resulted in counter responses to the aggregate size which were smaller than the actual aggregate size. Neis et al. (20) presented similar results for the particle size distribution of a suspension of *Bacillus Cereus* in 0.25 M NaCl.

Measuring aggregate size distribution with an electronic particle counter appears to have two distinct liabilities, both of which are related to the aggregate porosity. First, the electronic counter measures only the particulate matter (treated as a coalesced solid sphere) within a floc, whereas microscopic observation measures floc size including the enclosed electrolyte. The size of the coalesced particulate matter is obviously not comparable with the total visual floc size. Second, the calibration of the counter with monodisperse, impermeable singlets does not permit the direct measurement of aggregate volume distributions, since the aggregate porosity causes a counter response to the aggregate particulate matter which is smaller than justified by the actual particulate content. Thus, while the traditional view has been that the particulate matter can be treated as equal in size to a coalesced singlet of the same volume, the distribution of particulate matter throughout the aggregate causes a reduced counter response.

In spite of these difficulties, the electronic counter-multi-channel analyzer technique offers the potential for precise quantitative measurement of the flocculation of colloidal particles, provided that compensations for aggregate porosity are made. The following paragraphs present suggested improvements to the normal operation of the electronic counter-PHA-MCA in the measurement of aggregate size distributions.

Theory of Electronic Particle Counting

The operation of the Coulter counter-PHA-MCA in counting and sizing singlets has been thoroughly developed (6, 9, 12-15). The resistance change caused by the passage of a cylindrical particle through the measuring aperture is expressed:

$$\Delta R = (4 \rho_p / \pi D^4) \frac{d^3}{[1.5 / (1 - \rho_p / \rho)] - (d^2 / aD^2)} \quad (1)$$

where ρ_p = resistivity of electrolyte, ρ = resistivity of particle, D = aperture diameter, d = diameter of equivalent spherical particle, and a = shape coefficient.

The response to a singlet is directly proportional to the particle volume, except as modified by the second term in the denominator. Both Kubitschek (7, 8) and Wachtel and LaMer (9) found that d/D should not exceed 0.4 to minimize aperture blockage and preserve linearity of response.

For singlets, the relationship between the particle diameters (d_i and d_j) and the corresponding storage channels in the MCA (C_i and C_j) is

$$d_j = d_i y^{(C_j - C_i) / \Delta C} \quad (2)$$

where y = logbase used in the storage of voltage pulses produced by particle passage.

If d_i , C_i , C_j are known from zeroing experiments, then d_j is readily computed, provided that the particle is not an aggregate.

In the case of aggregates, however, these equations cannot be utilized because of the porosity of the aggregate itself. When a large aggregate of tightly bound singlets (1 μm in diameter) passes through a small (11 μm) or medium (30 μm) aperture, the aggregate tends to feather itself along the streamlines of the rapidly flowing sample volume. This elongation of the aggregate as it passes through the aperture results in a pulse having both height and width. Although the pulse height can be calibrated with monodisperse polystyrene latex particles, the pulse width goes uncalibrated. A similar result was noted by Mattern et al. (6) in their analysis of coincidence passage by singlet particles. Figure 1A depicts the critical volume in which the particle size is measured. Figures 1B and C show that the separation distance of two particles during coincident transit of the critical volume determines the relative pulse height and width. For small tightly bound aggregates, the pulse height should be directly proportional to the number of singlets in the aggregate. However, as the porosity increases and the aggregates elongate within the critical volume, the pulse width increases at the expense of pulse height.

A second problem occurs when a large aggregate passes through a medium (30 μm) or large (70 μm) aperture. If the porosity of the aggregate is large, then the aggregate sizing system (aperture, current, and amplification) is required to size and sum the many smaller pulses created by the primary particles which comprise the total aggregate. However, only the small 11- μm aperture is able to precisely detect and size singlets (1 μm in diameter); the larger 30- and 70- μm apertures only detect tightly aggregated singlet cells, and thus the system response is only a partial response to the total particulate volume within the aggregate. Neis et al. (20) recorded these effects as increases in the calibration factor during the course of coagulation, the calibration factor being the ratio of actual particulate volume to Coulter counter measured volume.

Proposed Modification to Theory for Aggregate Passage

To compensate for the effect of aggregate porosity upon the measured volume following flocculation, determinations of

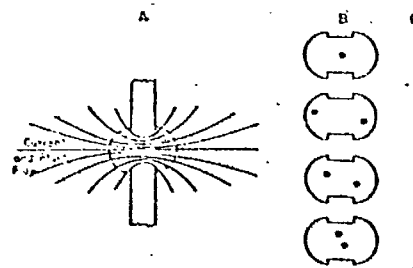


Figure 1. A: schematic representation of aperture, current density lines, and critical volume. B: particle separation distances within critical volume. C: resulting voltage pulses. Adapted from Mattern et al. (6)

aggregate porosity, as a function of the number of primary particles within an aggregate, were made either from calculations or from literature survey. These porosity values are summarized in Table II.

Some authors have attributed high porosity values to electrostatic repulsion between primary particles, a condition ameliorated by the adsorption of cationic coagulant to the negative colloidal surface and by the continuous agitation of the suspension during flocculation. Nevertheless, colloid-coagulant systems do produce open porous flocs, as observed via electron microscopy.

Figure 2 depicts a smooth curve of porosity vs. number of singlets per aggregate, drawn from the data of Table II so that two conditions are satisfied: For aggregates with less than eight singlets, the curve passes through the calculated porosity values; for larger aggregates, the curve is asymptotic to the porosity value between 0.50 and 0.95 which enables a conservation of volume condition to be met between unflocculated and flocculated state.

The shape of the curve relating the calculated porosity f to the number of cells per aggregate n suggests an exponential relationship of the form

$$n = ab^f \quad (3)$$

Table II. Typical Value of Aggregate Porosity as Function of Number of Singlets per Aggregate and Singlet Diameter

Singlets/aggregate	Configuration	Porosity	Ref
2	Linear	0.20	
3	Linear-triangular	0.25-0.26	
4	Linear-tetrahedral	0.27-0.29	
8	Cubic-rhombohedral	0.26-0.48	(21)
	Coarse sand	0.39-0.41	(22)
	Medium sand	0.41-0.48	(22)
	Fine sand	0.44-0.49	(22)
	Fine sandy loam	0.50-0.54	(22)
	$d \leq 20 \mu\text{m}$	0.50	(23)
	$d \leq 2 \mu\text{m}$	0.95	(23)
Silica powder	$d \leq 21 \mu\text{m}$	0.38	(24)
Silica powder	$4 \leq 16 \mu\text{m}$	0.43	(24)
Silica powder	$d \leq 6 \mu\text{m}$	0.38	(24)
Silica powder	$d \leq 16 \mu\text{m}$	0.43	(24)
Silica powder	$d \leq 6 \mu\text{m}$	0.75	(24)
Silica powder	$d \leq 2.3 \mu\text{m}$	0.89	(24)
Silica powder	$d \leq 5 \mu\text{m}$	0.71	(25)
Clay and alum	$d \leq 15 \mu\text{m}$	0.74-0.99	(18)

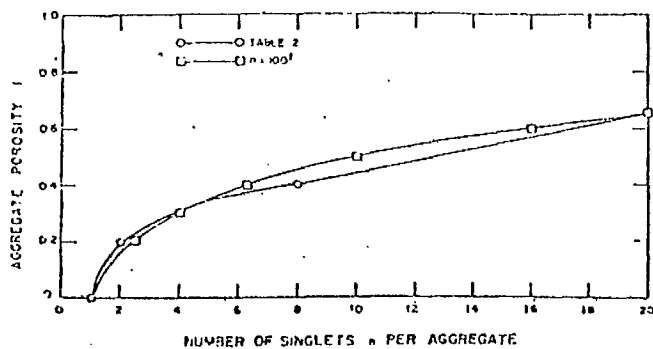


Figure 2. Aggregate porosity as function of number of singlets per aggregate

Since $n = 1$ at $f = 0$, $a = 1$. Further calculation provides a best fit when $b = 100$, yielding

$$n = 100^f$$

$$f = 0.5 \log n \quad (4)$$

During subsequent experiments an asymptotic porosity value of 0.69 was found to provide conservation of volume of the total suspended particulate matter between the unflocculated and flocculated state.

The formation factor F is defined as the ratio of the resistivity of the porous material, ρ_f , saturated with an electrolyte to the bulk resistivity of the same electrolyte, ρ_0 :

$$F = \rho_f / \rho_0$$

Archie (26) has determined an empirical relationship between porosity and formation factor which applies to most porous materials:

$$F = \rho_f / \rho_0 = f^{-m} \quad (5)$$

where $m = 2.0$ for clean sands, and slightly less than 2.0 for all other materials, i.e., $m \approx 1.9$.

Letting $m = 1.9$ for the aggregates and substituting Equation 4 into Equation 5 yields

$$\rho_f = \rho_0 (0.5 \log n)^{-1.9} \quad (6)$$

As the aggregate size increases, larger apertures must be used to maintain d/D less than 0.4, and d^2/aD^2 insignificant. Substituting Equation 6 into Equation 1 yields:

$$\Delta R = 4 \rho_0 d^3 [1 - (0.5 \log n)^{1.9}] / 1.5 \pi D^4 \quad (7)$$

In Equation 7 the response ΔR of the Coulter counter to the aggregate passage is a function of two unknowns: d , the equivalent spherical diameter of the aggregate, and n , the number of singlets per aggregate. However,

$$n = (\pi d^3 / 6) / (\pi d_0^3 / 6) \quad (8)$$

where d_0 = singlet diameter.

Therefore

$$\Delta R = 4 \rho_0 d^3 [1 - 1.5 \log (d/d_0)]^{1.9} / 1.5 \pi D^4 \quad (9)$$

Theoretically, for $d \leq d_0$

$$f = 1.5 \log (d/d_0) = 0$$

and

$$\Delta R = 4 \rho_0 d^3 / 1.5 \pi D^4 \quad (10)$$

In this case the electronic counter response is directly proportional to the particle diameter d .

For $d_0 < d < 2.9 d_0$ ($1 < n < 24$)

$$f = 1.5 \log (d/d_0) = 0.69$$

$$[1 - [1.5 \log (d/d_0)]^{1.9}] = 0.50$$

and

$$\Delta R = 2 \rho_0 d^3 / 1.5 \pi D^4 \quad (11)$$

Finally, for $d > 2.9 d_0$ ($n > 24$)

$$f = 1.5 \log (d/d_0) = 0.69$$

$$[1 - [1.5 \log (d/d_0)]^{1.9}] = 0.50$$

and

$$\Delta R = 2 \rho_0 d^3 / 1.5 \pi D^4 \quad (12)$$

Consequently, in the intermediate size range the response of the electronic counter to aggregate particulate matter does not increase linearly with the increase in aggregate particulate

matter. After the limiting porosity value ($f = 0.69$) is reached, the response again increases linearly with the aggregate size.

When an aggregate of diameter d_j passes through the aperture, the normal counter response, given by Equation 10, must be modified to compensate for the aggregate porosity so that:

$$\Delta R_j = 4 \rho_0 d_j^3 [1 - [1.5 \log (d_j/d_0)]^{1.9}] / 1.5 \pi D^4 \quad (13)$$

$$\Delta R_j = \Delta R_{d_0} y^{(C_j - C_{d_0})} = 4 \rho_0 (d_0)^3 y^{(C_j - C_{d_0})} / 1.5 \pi D^4 \quad (14)$$

Therefore:

$$d_j^3 [1 - [1.5 \log (d_j/d_0)]^{1.9}] = (d_0^3) y^{(C_j - C_{d_0})} \quad (15)$$

In Equation 15, d_0 , y , C_j , and C_{d_0} are known; therefore, d_j can be calculated via an iterative technique using an initial estimate that:

$$d_j \geq d_0 y^{(C_j - C_{d_0})/3} \quad (16)$$

The porosity factor $[1 - [1.5 \log (d_j/d_0)]^{1.9}]$ decreases until it reaches 0.5, which corresponds to the asymptotic value of the porosity for large aggregates, $f = 0.69$. The overall effect at a porosity of 0.69 is to increase the aggregate diameter 25% above that recorded by the Coulter counter.

Experimental Materials and Methods

A series of polyethyleneimine (PEI) polymers was selected as coagulants because of the range of molecular weights available from 600 to 60 000, corresponding to 14–1400 monomer (C_2NH_5) units. PEI in solution functions as a cationic polyelectrolyte strongly attracted to negatively charged colloids (27). The colloid was *E. coli* strain CR 63, grown in batch culture to a cell concentration of $2.5 (+0.5) \times 10^7$ cells/mL in the following medium:

Ingredient	g/L
Casamino acid (acid hydrolyzed casein)	1.20
Glucose	1.00
NH ₄ Cl	1.00
KH ₂ PO ₄	0.10
Collidine-HCl buffer, pH 7.0	50 ml/L
MgSO ₄ , 1 M	2 ml/L
FeCl ₃ , 10 ⁻³ M	1 ml/L

At the end of log phase growth, the relatively monodisperse coliform has a cylindrical shape: 0.8 μ m in diameter, 2–3 μ m in length, with a mean equivalent spherical diameter of 1.3 μ m.

Two serial dilutions of 10:1 of the initial cell concentration resulted in 2.5×10^5 cells/mL or 1.25×10^4 cells/50 μ L. At this concentration the 11- μ m aperture will give a true count of cell concentration without requiring coincidence corrections (6). The ionic strength of the growth medium and the dilutant was 0.06 M NaCl, the temperature 25 °C, and the pH 7.0 (± 0.1).

Following removal from the chemostat, the *E. coli* suspension (300 mL of 2.5×10^7 cells/mL) was rapidly mixed in a stirrer-reactor assembly (J) at a mean temporal velocity gradient $G = 190 \text{ s}^{-1}$ for 2 min while simultaneously adding 100 mL of PEI solution. Following rapid mix the flocculating suspension was stirred at a velocity gradient of 20 s^{-1} for 4 h. Particle size distributions were recorded every 60 min during the 4-h flocculation period, primarily to determine if the aggregate would reach an equilibrium size determined by the imposed velocity gradient and the PEI molecular weight, but also to verify the proposed modifications to normal electronic counter operation over a wide range of aggregate sizes.

The current and amplification settings of the Model B Coulter counter were determined for three different aperture

diameters (11, 30, and 70 μ m) by passing suspensions of monodisperse polystyrene latex in 0.06 M NaCl through the aperture. The settings, summarized in Table III, provide strong signal-to-noise ratios and maintain the ratio of particle diameter d to aperture diameter D greater than 0.07 and less than 0.20.

A voltage pulse generator was used with the Nuclear Data Model 555 pulse height analyzer (PHA) and multichannel analyzer (MCA) to determine the coarse and fine gain settings so that the logbase of input signals remained constant over the full range of channels, i.e., from channel 1 to 128. Varying the frequency of the voltage pulse within the recovery time of the electronic circuitry did not shift the channel of record.

A detailed particle size distribution could be obtained by using 80 channels of data from the 11- μ m aperture, 80 channels of data from the 30- μ m aperture, and 100 channels of data from the 70- μ m aperture. All 128 channels could not be utilized because of overlap between the 11- and 30- μ m apertures, and between the 30- and 70- μ m apertures. Bacteria of equivalent spherical diameter less than 1.13 μ m could not be detected by the 11- μ m aperture because of background electronic noise at this low signal level.

Prior to seeding the culture, the growth medium was filtered through 0.45- μ m Millipore filters to remove any large particulate matter. After culture growth, plate counts and hemacytometer counts were made to verify the accuracy of the Coulter counter measurements. As was previously noted by Mattern et al. (6), the counts from the Coulter counter had better reproducibility than either of the other techniques.

Samples of the flocculating *E. coli* suspension were withdrawn from the stirrer-reactor with a 2-mm bore pipet to prevent aggregate breakup, and then diluted with 0.06 M filtered NaCl. The dilution ratio depended upon the number of aggregates per unit volume, i.e., the reactor suspension was diluted only to the degree necessary to ensure significance of count and adequate relaxation time of the electronic circuitry. Since little difference exists in densities between the *E. coli* cells and the suspending electrolyte, sedimentation of the particle aggregates during the time required to make a count and size distribution was negligible. The aggregates did not appear to fragment as they passed through the aperture, in spite of the high shear forces encountered there (17).

The smaller apertures (11 and 30 μ m) were prone to blocking by the aggregated bacterial cells. Generally, blockages could be cleared with a small paint brush; the more difficult cases were cleared by briefly immersing (1 s) the entire aperture tube into the bath of an ultrasonic vibrator. Occasionally, single cells would adhere to the sides of the aperture, resulting in an effective reduction in the aperture size, and therefore increased pulse heights. By using a stopwatch to record the sampling time, such minor blockages were immediately detected, and the aperture could be cleared with the ultrasonic vibrator.

Using the calibration techniques discussed earlier, aggregate size distributions were prepared from the Coulter counter data.

Table III. Summary of Calibration Data for Coulter Counter

Aperture diam, μ m	Particle diam, μ m	Counter settings		Peak channel	Logbase
		Amp	Current		
11	1.3	0.5	8	38	1.024
	2.0	0.5	3	94	
30	2.0	2.0	4	24	1.045
	5.7	2.0	4	95	
70	5.7	8.0	4	20	1.032
	9.5	8.0	4	70	

taken each hour after addition of the PEI. The aggregate count in each channel C_i was converted to aggregate count at diameter d_i via a computer program utilizing Equations 15 and 16. This aggregate count, divided by the diameter change corresponding to the size range stored in each channel, yielded the differential number distribution. Similarly, a differential volume distribution was prepared by dividing the aggregate volume by the log of the diameter change corresponding to the size range stored in each channel.

Experimental Results

Figure 3A reflects the change in the differential number distribution over a 4-h period of stirring at $G = 20 \text{ s}^{-1}$ when no polymer has been added. The peak in the particle number distribution occurs at the mean cell diameter $1.3 \mu\text{m}$. Cell aggregates are present, though in small concentrations. These aggregates are caused by bioflocculation, which increases with time because of the continuous release of extracellular biopolymers, and to coagulation by the 0.06 M NaCl dilutant. Figure 3B is the corresponding differential volume distribution when no polymer has been added.

Figure 4A is the differential number distribution for *E. coli* cells flocculated with the optimum dose (5.0 mg/L) of the low-molecular-weight PEI 6 ($\text{MW} = 600$). The extent of flocculation increases continually with agitation at $G = 20 \text{ s}^{-1}$. At this molecular weight and velocity gradient, most aggregates are concentrated in the range $1\text{--}4 \mu\text{m}$, with the number

of the latter increasing with time as the number of the former decreases. Figure 4B indicates the shift in the volume distribution caused by the addition of cationic polymer PEI 6.

Figure 5A is the differential number distribution for *E. coli* cells flocculated with the optimum dose (5.0 mg/L) of PEI 18 ($\text{MW} = 1800$). Continuous growth of larger aggregates in the $8\text{--}12\text{-}\mu\text{m}$ range occurs at the expense of the smaller $1\text{--}4\text{-}\mu\text{m}$ aggregates. The presence of these larger aggregates indicates an increasing shear resistance with the higher-molecular-weight polymer species, since no aggregates in this size range occurred with PEI 6 or PEI 12. Figure 5B, the corresponding differential volume distribution, illustrates the shift in volume distribution from the initial distribution (singlet particles with diameters in the range $1\text{--}2 \mu\text{m}$) to the distribution after 60 min of flocculation (aggregates with diameters in the range $8\text{--}12 \mu\text{m}$, or 230–790 singlets/aggregate).

Finally, the effect of the cationic polymer PEI 600 ($\text{MW} = 60\,000$) upon the dispersed *E. coli* cells is shown in Figure 6A at the optimum polymer dose (0.5 mg/L). A dramatic decrease in the number of singlet cells (from 10^8 to 10^6 cells $\text{cm}^{-3}/\mu\text{m}$) and a dramatic increase in the size of the largest aggregate (greater than $12 \mu\text{m}$) are observed. The growth of very large aggregates occurs at the expense of small ($1\text{--}4 \mu\text{m}$) and medium ($4\text{--}8 \mu\text{m}$) sized aggregates, both of which are an order of magnitude less in number than when flocculated with PEI 12 or PEI 18. The shift in the differential volume distribution to aggregates in the $10\text{--}20\text{-}\mu\text{m}$ range (1540–3640 singlets/aggregate) is given in Figure 6B.

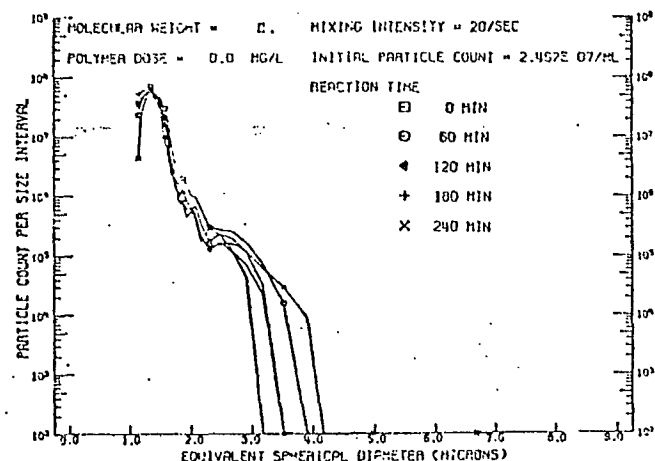


Figure 3A. Differential number distribution of *E. coli* aggregates with added flocculent

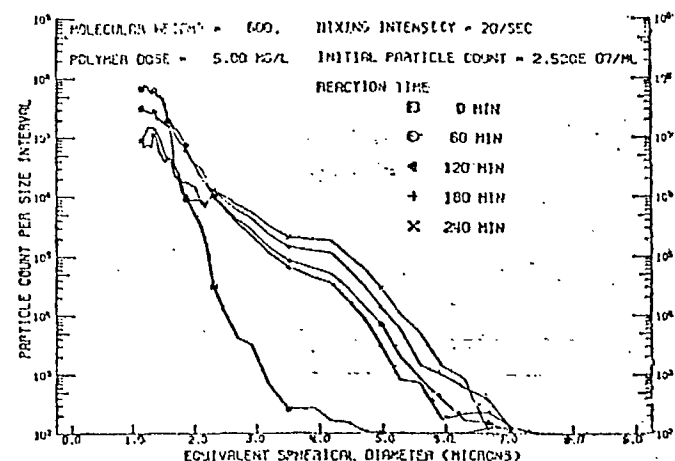


Figure 4A. Differential number distribution of *E. coli* aggregates at optimum dose of PEI 6 flocculent

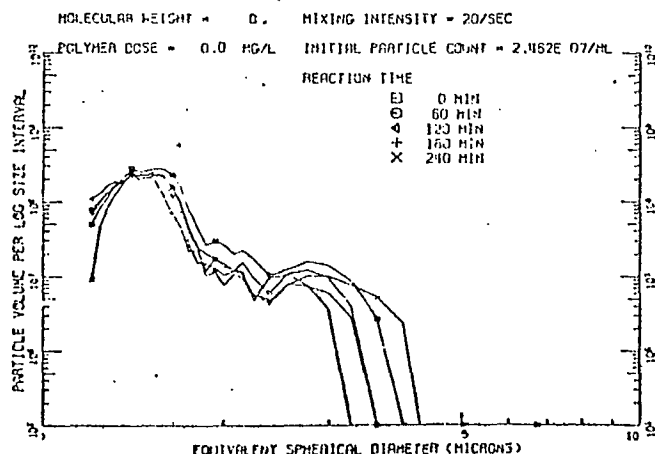


Figure 3B. Differential volume distribution of *E. coli* aggregates with no added flocculent

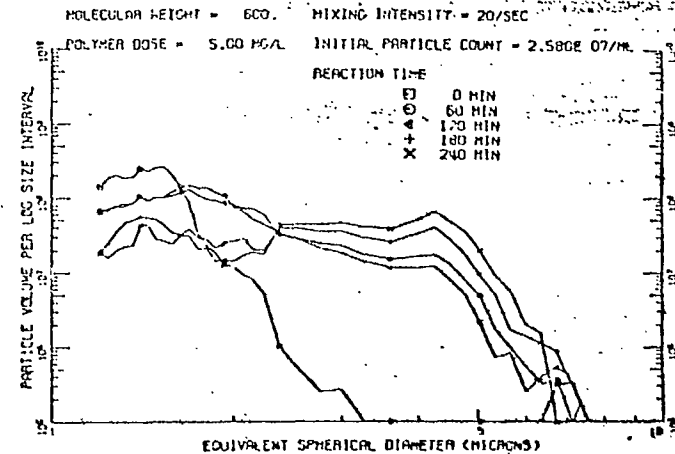


Figure 4B. Differential volume distribution of *E. coli* aggregates at optimum dose of PEI 6 flocculent

When the *E. coli* suspension was continuously stirred without polymer addition, the total particulate volume as measured by the Coulter counter-PHA-MCA remained constant within the experimental limitations ($\pm 5\%$) of the sampling and measuring technique. However, as aggregates were formed because of the addition of cationic polymer, the measured total particulate volume decreased in spite of the agitation ($G = 20 \text{ s}^{-1}$) which prevented aggregate sedimentation. Losses to the sides of the stirrer-reactor did not occur because of the very smooth polyethylene and Teflon surfaces and the continuous stirring. The recorded decrease in the volume of suspended matter is attributed to the inability of the electronic circuitry to record the width of the pulse produced as the aggregate passes through the aperture, and to the inability of the larger aperture combinations to precisely size and sum the many singlet particles which comprise the total aggregate volume. Both of these phenomena can be related to the amount of electrolyte contained within the floc particle, and thus to the porosity of the aggregate. The application of the theoretically derived porosity correction to the basic Coulter counter-PHA-MCA data resulted in conservation of volume between the unflocculated and flocculated state of the suspended matter. This porosity correction does not measure the actual porosity of large aggregates, but rather enables the researcher to evaluate the effect of this aggregate porosity upon the response of the electronic counter. The porosity correction, as expressed in Equations 13, 15, and 16, was experimentally verified in flocculation conditions extending

from monodisperse size distributions ($n = 1$) to large aggregates ($n \leq 4000$).

Summary

To measure a constant volume of suspended particulate matter in a coagulating suspension, modification of the normal operating procedure for electronic particle sizing is required. This modification results in considering the effects of aggregate porosity upon the electronic response to aggregate passage through the aperture. The equation for the electronic response to singlet passage was modified to account for aggregate porosity with the porosity increasing with aggregate size up to an asymptotic value. This theoretical correction was then verified experimentally using *E. coli* cells as the suspended colloid and the cationic polymer, polyethyleneimine, as the coagulant.

The electronic counter responds only to the particulate matter within a floc; consequently, the equivalent spherical diameter so determined represents that of a coalesced sphere. For this reason the floc size recorded via electronic particle counting cannot be directly correlated with the floc size recorded microscopically.

By recording the complete size distribution from singlet particle to the largest aggregate, the conservation of volume condition can be utilized to determine the effect of aggregate porosity on counter response. Once this correction is made, the Coulter counter-PHA-MCA can be effectively utilized to evaluate the flocculation process as it occurs in the reactor basin.

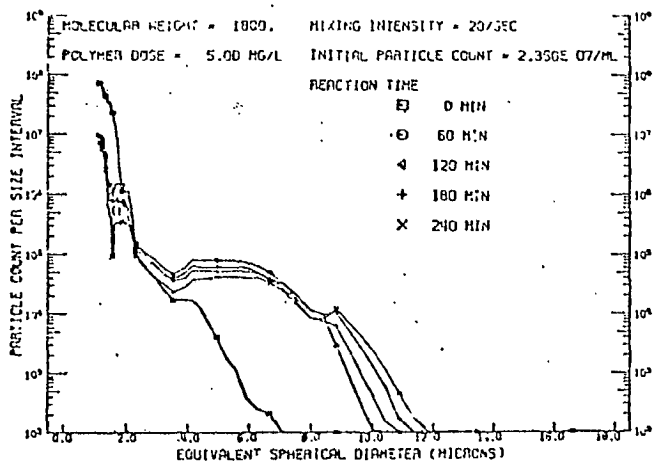


Figure 5A. Differential number distribution of *E. coli* aggregates at optimum dose of PEI 18 flocculent

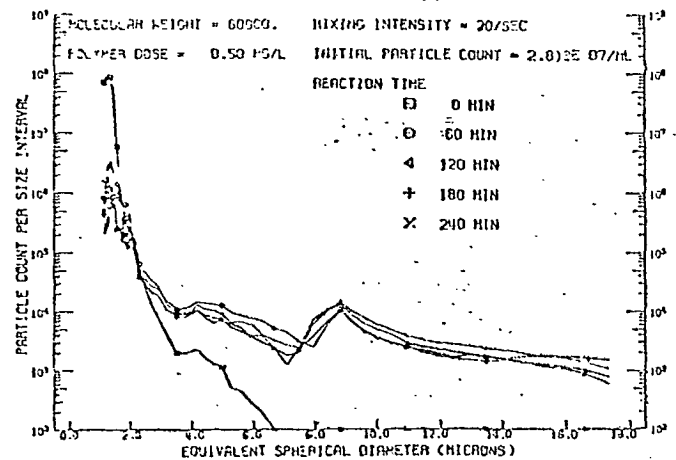


Figure 6A. Differential number distribution of *E. coli* aggregates at optimum dose of PEI 600 flocculent

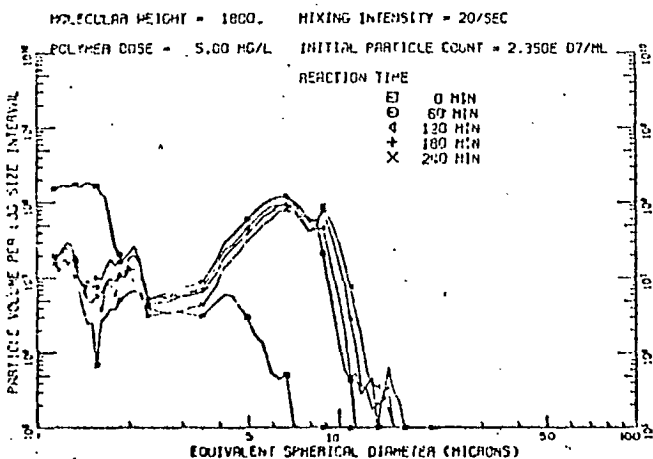


Figure 5B. Differential volume distribution of *E. coli* aggregates at optimum dose of PEI 18 flocculent

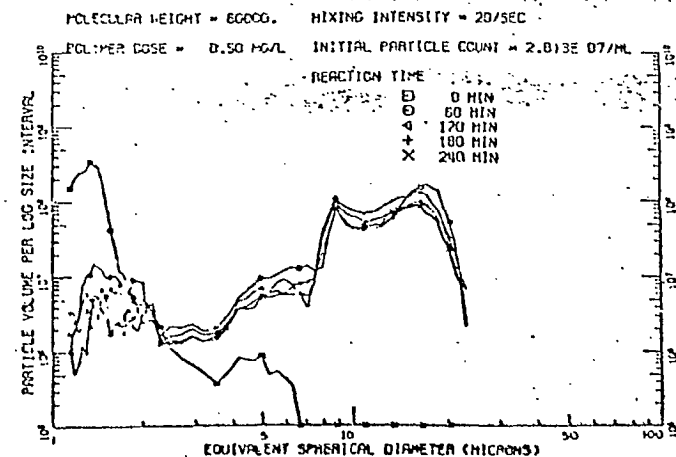


Figure 6B. Differential volume distribution of *E. coli* aggregates at optimum dose of PEI 600 flocculent

Literature Cited

- (1) "Particle Counting and Sizing Analysis System", Pacific Scientific Co., California, 1975.
- (2) LaMer, V. K., Smellie, R. H., Lee, P. K., *J. Colloid Sci.*, 12, 566 (1957).
- (3) O'Melia, C. R., Stumm, W., *J. Colloid Interface Sci.*, 23, 437 (1967).
- (4) Treweek, G. P., PhD thesis, California Institute of Technology, Pasadena, Calif., 1975.
- (5) O'Melia, C. R., "Coagulation and Flocculation", in "Physico-chemical Processes for Water Quality Control", W. J. Weber, Ed., Wiley-Interscience, New York, N.Y., 1972.
- (6) Mattern, C. P., Brackett, F. S., Olson, B. J., *J. Appl. Physiol.*, 10, 59 (1957).
- (7) Kubitschek, H. E., *Nature*, 182, 234 (1958).
- (8) Kubitschek, H. E., *Research (London)*, 13, 128 (1960).
- (9) Wachtel, R. E., LaMer, V. K., *J. Colloid Sci.*, 17, 531 (1962).
- (10) Coulter, W. H., *Proc. Nat. Electron. Conf.*, 12, 1034 (1955).
- (11) Higuchi, W. I., Okada, R., Lemberger, A. P., *J. Pharm. Sci.*, 51, 683 (1962).
- (12) Morgan, J. J., Birkner, F. B., "Flocculation Behavior of Dilute Clay-Polymer Systems", Progress Rep. WP 00912-02, USPHS, Keck Lab, Caltech, Pasadena, Calif., 1966.
- (13) Birkner, F. B., Morgan, J. J., *J. Am. Water Works Assoc.*, 60, 175 (1968).
- (14) Ham, R. K., Christman, R. F., *Proc. Am. Soc. Civil Eng.*, 95, 481 (1969).
- (15) TeKippe, R. J., Ham, R. K., *J. Am. Water Works Assoc.*, 62, 594 (1970); *ibid.*, p 620.
- (16) Camp, T. R., *ibid.*, 60, 656 (1968).
- (17) Hannah, S. A., Cohen, J. M., Robeck, G. G., *ibid.*, 59, 843 (1967).
- (18) Camp, T. R., *J. Sanit. Eng. Div., Am. Soc. Civ. Eng.*, 95, 1210 (1969).
- (19) Ham, R. K., PhD thesis, University of Washington, Seattle, Wash., 1967.
- (20) Neis, U., Eppler, B., Hahn, H., "Quantitative Analysis of Coagulation Processes in Aqueous Systems: An Application of the Coulter Counter Technique", unpublished paper, 1974.
- (21) Graton, L. C., Fraser, H. J., *J. Geol.*, 43, 785 (1935).
- (22) Muskat, M., "The Flow of Homogeneous Fluids Through Porous Media", McGraw-Hill, New York, N.Y., 1937.
- (23) Terzaghi, K., *Eng. News Rec.*, 95, 912 (1925).
- (24) Shapiro, I., Kolthoff, I., *J. Phys. Colloid Chem.*, 52, 1020 (1948).
- (25) Dixon, J. K., LaMer, V. K., Linford, H. R., *J. Water Pollut. Control Fed.*, 39, 647 (1967).
- (26) Archie, G. E., *Trans. Am. Inst. Min. Metall. Eng.*, 146, 54 (1942).
- (27) "PEI Polymers", Dow Chemical Co., Midland, Mich., 1974.

Received for review September 20, 1976. Accepted February 28, 1977.